

443 Physiological and myopic ocular biometry

Wednesday, May 10, 2017 11:00 AM–12:45 PM

Exhibit/Poster Hall Poster Session

Program #/Board # Range: 4423–4440/A0401–A0418

Organizing Section: Anatomy and Pathology/Oncology

Program Number: 4423 **Poster Board Number:** A0401

Presentation Time: 11:00 AM–12:45 PM

Peripheral refraction and peripheral eye length in myopic children in the BLINK study

Donald O. Mutti¹, Loraine T. Sinnott¹, Kathleen Reuter¹, Maria Walker², David A. Berntsen², Lisa A. Jones-Jordan¹, Jeffrey J. Walline¹. ¹College of Optometry, Ohio State University, Columbus, OH; ²College of Optometry, University of Houston, Houston, TX.

Purpose: This analysis describes the relationship between peripheral refractive error and peripheral eye length in myopic children.

Methods: Subjects were 294 myopic children with a mean age (\pm SD) of 10.3 \pm 1.2 years. Central spherical-equivalent (SE) refractive error was the mean of 5 measurements in primary gaze using a Grand Seiko WAM-5500 autorefractor following instillation of two drops of tropicamide 1%. Peripheral SE refractive error was the mean of 5 measurements assessed at 20°, 30°, and 40° nasal and temporal retina and 20°, 30° superior and inferior retina. Eye length was the mean of 5 measurements made with a Haag-Streit Lenstar LS-900 biometer in primary gaze, then at 20° and 30° laterally and vertically.

Results: Central SE refractive error was -2.42 ± 1.03 D and central eye length was 24.48 ± 0.81 mm. Peripheral SE refractive error became relatively more hyperopic away from the fovea laterally (by $+1.82 \pm 1.44$ D at 40° temporal retina) but was relatively more myopic in the vertical meridian (by -0.59 ± 1.20 D at 30° inferior retina). Consistent with the relative hyperopic shift in the lateral periphery, eye length decreased by as much as -0.76 ± 0.24 mm at 30° temporal retina. The relative myopia vertically was associated with smaller decreases in eye length (-0.43 ± 0.22 mm at 30° inferior retina). Correlations between relative peripheral refractive error and relative peripheral eye length were on the order of -0.51 to -0.60 laterally and -0.33 to -0.59 vertically (all $p < 0.001$). The more myopic the foveal refractive error, the steeper the peripheral retina, both laterally and vertically.

Conclusions: The peripheral refractive errors and eye lengths of myopic children are similar to those described for myopic adults, suggesting little change in relationship over time. Although significantly correlated, the two variables are not interchangeable and should be analyzed separately.

Commercial Relationships: Donald O. Mutti, Loraine T. Sinnott, Bausch & Lomb (F); Kathleen Reuter, Bausch & Lomb (F); Maria Walker, Bausch & Lomb (F); David A. Berntsen, Bausch & Lomb (F); Lisa A. Jones-Jordan, Bausch & Lomb (F); Jeffrey J. Walline, Bausch & Lomb (F)

Support: NIH NEI U10EY023210, U10EY023208, U10EY023204, U10EY023206

Clinical Trial: NCT02255474

Program Number: 4424 **Poster Board Number:** A0402

Presentation Time: 11:00 AM–12:45 PM

Ocular growth during infancy and early childhood

Ian Cunningham, Arvind Chandna, Sylwia Migas. Ophthalmology, Alder Hey Children's NHS Foundation Trust, Liverpool, United Kingdom.

Purpose: There is limited knowledge of normal ocular growth during early childhood. Such information would make an important contribution towards management of childhood conditions such as

myopia, cataract and glaucoma. We performed a prospective, cross-sectional, clinical study to measure ocular growth in a large cohort of infants and young children.

Methods: 330 children (aged 7 weeks to 7 years) with no ocular problems, undergoing routine surgery for non-ophthalmic related conditions were recruited. All measurements, carried out by a single clinical researcher, were performed during general anaesthesia and before the operating procedure. Standard, direct corneal applanation instruments were used to ensure accuracy. Axial length, lens thickness, anterior and vitreous chamber depth measurements were obtained for both eyes of each subject.

Results: The right eyes of the participants were included in the final analysis. The best fit to the data was obtained using the least-squares method. Several functional models were investigated, including increasing forms of the exponential decay. It was concluded, that the growth of the axial length for ages between 7 weeks to 7 years is best described by the natural logarithm function with two coefficients. The bootstrap method was used to calculate the confidence bounds for the fitted coefficients at 95% confidence level.

The overall ocular growth pattern is characterised by a rapid growth in the first year of life, followed by a steady growth throughout the measured study range. AL increased from 16.63mm (16.24, 17.03mm, 95% CI) to 22.58mm (21.66, 23.45mm) at age 7 years. ACD increased from 2.80mm (2.63, 2.97mm) to 3.58mm (3.26, 3.90mm). VCD increased from 10.41mm (9.92, 10.86mm) to 14.67 (13.73, 15.51mm). LT remained similar at 3.84mm (3.82, 3.88mm) to 3.82mm (3.78, 3.87mm).

Conclusions: This is the largest dataset and the only study measuring ocular growth using direct methods. We present normal ocular growth measurements and their functional forms. The rapid growth of the eye in early childhood is contributed largely by growth of the vitreous chamber, which mimics the axial length growth pattern. Our measurement of normal ocular growth should be applicable in clinical setting to increase the understanding of impact of childhood ocular conditions on ocular growth.

Commercial Relationships: Ian Cunningham, None; Arvind Chandna, None; Sylwia Migas, None

Program Number: 4425 **Poster Board Number:** A0403

Presentation Time: 11:00 AM–12:45 PM

Ten-year change of refractive error, anterior chamber depth and axial length in southern Chinese children

Zhixi Li¹, Zhuoting Zhu¹, Xiaohu Ding¹, Mingguang He^{1,2}. ¹prevention of blindness, Zhongshan Ophthalmic Center, Sun Yat-sen University, Guangzhou, China; ²Centre for Eye Research Australia, University of Melbourne, Melbourne, VIC, Australia.

Purpose: To evaluate changes in refractive errors (REs), anterior chamber depth (ACD) and axial length (AL) among southern Chinese children over a ten year period.

Methods: The first-born twins aged 7 to 15 years old in baseline (2006) from Guangzhou Twin Eye Study with annually visits from 2006 to 2016 were included in this study. Children underwent noninvasive partial-coherence laser interferometry (IOLMaster) before pupil dilation and cycloplegic autorefraction.

Results: A total of 637 participants underwent comprehensive examinations from 2006 to 2016 (2006 mean [SD] age, 10.66 [2.3] years; 51.3% female). In the longitudinal data, linear mixed models were used to explore changes in outcomes over time. Myopic SE ($P < .001$) and AL ($P < .001$) increased at 0.29 diopter/y (95% CI, 0.28 to 0.29) and 0.16 mm/y (95% CI, 0.16 to 0.18) respectively. And females were more likely to get more myopic and longer axial length than males (both $P < 0.001$). There was no significant change of ACD over the follow up period (0.246).

Conclusions: This study shows that the important longitudinal changes of RE, ACD and AL in southern Chinese children and myopia is very prevalent among Chinese children.

Commercial Relationships: Zhixi Li, None; Zhuoting Zhu, None; Xiaohu Ding, None; Mingguang He, None

Support: Fundamental Research Funds of the State Key Laboratory in Ophthalmology, National Natural Science Foundation of China 81125007, Science and Technology Planning Project of Guangdong Province, China 2013B20400003

Program Number: 4426 **Poster Board Number:** A0404

Presentation Time: 11:00 AM–12:45 PM

Quantitative-ultrasound assessment of the myopic sclera in the guinea pig

Jonathan Mamou¹, Ronald H. Silverman², Sally A. McFadden³, Quan V. Hoang^{2,4}. ¹Lizzi Ctr for Biomedical Engineering, Riverside Research, New York, NY; ²Department of Ophthalmology, Columbia University Medical Center, New York, NY; ³Vision Sciences Group, Faculty of Science and IT, School of Psychology, University of Newcastle, Newcastle, NSW, Australia; ⁴Singapore Eye Research Institute, Singapore National Eye Centre, Singapore, Singapore.

Purpose: Quantitative ultrasound (QUS) permits estimation of QUS parameters associated with tissue microstructure and organization. In this study, QUS parameters were obtained using 80-MHz ultrasound (US) images from the posterior sclera in myopic guinea pigs (GPs). We hypothesize that QUS may provide a new and quantitative contrast mechanism that could ultimately assess ocular biomechanical properties *in vivo*.

Methods: US radiofrequency data were collected using a broadband 80-MHz transducer (Figs. 1a,b) from both eyes of GPs that had undergone form deprivation in the right eye (5–20 days). Intact, normotensive eyes were immersed, “levitated” in Dulbecco’s phosphate buffered saline and anchored in a nearly *in vivo* anatomic position with partial thickness corneal sutures (Fig. 1c). With the transducer aimed at the posterior pole of the eye, a 2D scan centered at the optic nerve was acquired and the data were processed to derive several QUS parameters.

Results: Figure 1d depicts results obtained from an animal that had -7.24D of induced relative myopia (left +6.72D, right -0.52D). Specifically, it shows conventional US images augmented with color-coded information corresponding to the value of the effective scatterer diameter (ESD), which is a QUS parameter providing the effective size of the structures responsible for US scattering. A striking quantitative contrast is visible, with ESD values lower in the myopic right eye ($9.0 \pm 0.50 \mu\text{m}$) than in the contralateral control eye ($10.4 \pm 0.50 \mu\text{m}$, t-test, $p < 0.0001$).

Conclusions: This study establishes that QUS methods may be sensitive to changes occurring in the posterior sclera during myopia. For example, US scattering could be dominated by collagen fibrils and QUS methods and ESD could potentially be sensitive to these structural changes. QUS may provide a new means of quantitatively assessing myopia progression, severity, and treatment efficacy.

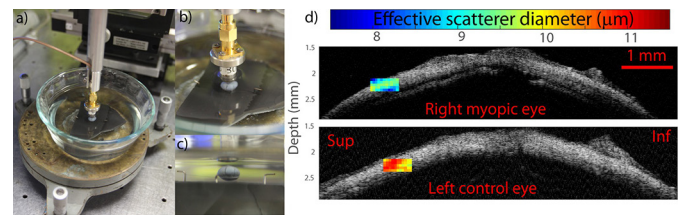


Figure 1: a) Photograph of the 80-MHz QUS experiments, b) 80-MHz transducer above the posterior eye surface, and c) eye “levitating” in solution with the sclera essentially under zero tension, mimicking *in vivo* conditions. QUS images obtained from the control (d, bottom) and myopic (d, top) eyes. The color-coded information is the effective scatterer diameter, which shows contrast between the myopic and control eyes.

Commercial Relationships: Jonathan Mamou, None; Ronald H. Silverman, None; Sally A. McFadden, None; Quan V. Hoang, None

Support: This work was supported in part by an unrestricted grant from Research to Prevent Blindness (RPB), NIH Core Grant P30EY019007, NIH Grant R21EB016117 (JM), Hunter Medical Research Institute HMRI G1400967 (SAM) and Career Development Awards from Research to Prevent Blindness (QVH), K08 Grant (QVH, 1 K08 EY023595, National Eye Institute, NIH) and philanthropic support from Joseph Connors (QVH).

Program Number: 4427 **Poster Board Number:** A0405

Presentation Time: 11:00 AM–12:45 PM

Time course of axial length changes in response to competing episodes of myopic and hyperopic defocus

Samaneh Delshad, Michael J. Collins, Scott A. Read, Stephen Vincent. Contact Lens & Visual Optics Laboratory, School of Optometry & Vision Science, Queensland University of Technology, Brisbane, QLD, Australia.

Purpose: To investigate the short-term changes in human axial length (AxL) in response to continuous and competing episodes of myopic and hyperopic defocus.

Methods: The right eye of 16 young adults was exposed to 60 min episodes of either continuous or competing myopic and hyperopic defocus (+3 D & -3 D), with the left eye optimally corrected to maintain far accommodation. During competing defocus, the eye was exposed to either 30 min or 15 min of alternating cycles of myopic and hyperopic defocus, with the order of lens wear reversed in separate sessions to assess the effects of defocus order. During each 60 min trial, the subjects watched a movie at 6 m in low photopic conditions. The right eye’s AxL was measured at baseline and then at 15 min intervals using Lenstar optical biometry. A binocular beam splitter periscope system was used to maintain distance fixation (left eye) and defocus exposure (right eye) during measurements.

Results: AxL underwent a greater magnitude of change during continuous defocus than during competing defocus. The maximum AxL change observed during continuous hyperopic defocus was $+7 \pm 2 \mu\text{m}$ of elongation ($p = 0.015$) and during continuous myopic defocus was $-8 \pm 2 \mu\text{m}$ of reduction in AxL ($p = 0.07$). When the eye was exposed to 30 min cycles of competing myopic and hyperopic defocus of equal duration, the opposing blur sessions cancelled each other and the eye was at near baseline levels following the final defocus session (final change from baseline, both $p > 0.05$). When the frequency of alternating cycles was 15 min, there was a slight AxL reduction after 60 min of myopic then hyperopic defocus, and hyperopic then myopic defocus, and were $-3 \pm 2 \mu\text{m}$ and $-4 \pm 2 \mu\text{m}$, respectively (final change from baseline, both $p > 0.05$) (Figure 1).

Conclusions: In the human eye, the AxL changes within minutes in response to short-term imposed myopic and hyperopic defocus. With competing defocus, at 30 min exposure frequencies, the effects of myopic and hyperopic blur largely cancel each other. At higher frequencies (15 min of alternating exposure), the effect on AxL of myopic defocus appears to be slightly more potent than hyperopic defocus.

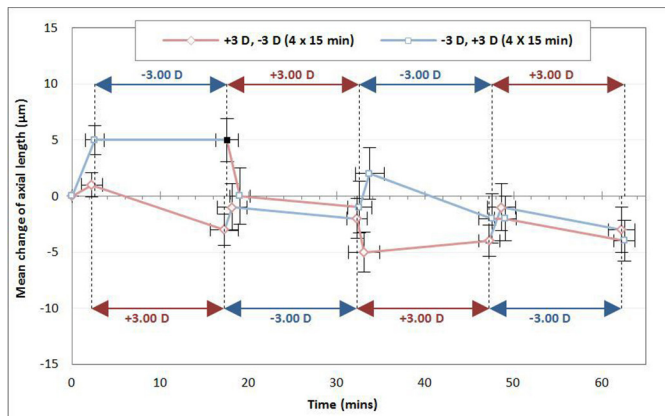


Figure 1. Plot of mean change in AxL from baseline during 60 min alternating cycles (15 min) of myopic then hyperopic defocus, and hyperopic then myopic defocus in all subjects. Solid symbol indicates significant mean difference from the baseline AxL.

Commercial Relationships: Samaneh Delshad, None; Michael J. Collins, None; Scott A. Read, None; Stephen Vincent, None

Program Number: 4428 **Poster Board Number:** A0406

Presentation Time: 11:00 AM–12:45 PM

Scleral, Choroidal and Retinal Thickness in Healthy Chinese Children Measured by Swept-source Optical Coherence Tomography

Xiangui He¹, Junjie Deng², Jiali Jin¹, Minzhi Lv¹, Jianfeng Zhu¹, Haidong Zou^{1,2}, Xun Xu^{1,2}. ¹Department of Preventative

Ophthalmology, Shanghai Eye Disease Prevention and Treatment Center, Shanghai, China; ²Department of Ophthalmology, Shanghai General Hospital, Shanghai Jiao Tong University, Shanghai, China.

Purpose: To explore the subfoveal scleral, choroidal and retinal thickness in healthy Chinese children with different refractive levels.

Methods: Cross-sectional study. A total of 810 children and adolescents aged 6 to 19 years were included. Each participant underwent a series of comprehensive ocular examinations, including swept-source optical coherence tomography (SS-OCT) and autorefractometry examinations after cycloplegia. The thicknesses of the sclera, choroid and retina were measured at the central fovea manually, and each was compared among children with different refractive levels. The independent factors of each layer were analyzed using stepwise multiple linear regression.

Results: The mean age of the 810 participants was 12.8±3.1 years. The mean subfoveal scleral thickness (SST), subfoveal choroidal thickness (SCT) and subfoveal retinal thickness (SRT) were 524±57 µm, 195±49 µm and 224±19 µm, respectively. Compared with emmetropes and hyperopes, myopes had a significantly thinner sclera and choroid (P<0.001). No significant difference (mean difference < 1 µm) was observed between emmetropes and hyperopes in the sclera, while in the choroid, a meaningful difference existed (mean difference 14 µm), however, it was not statistically significant. There was no significant difference in SRT between the myopes and emmetropes or between the emmetropes and hyperopes.

Among the myopic children, the SST and SCT decreased as the diopters of myopia decreased, while the SRT remained relatively stable. The SST (standard β=0.110) and SCT (standard β=0.063) as well as age, gender, and axial length (standard β=-0.673) were independently associated with spherical equivalent refraction (SER) in the regression model (R²=0.699, P<0.001). Older age, myopic-shifted SER, thicker SCT and thinner SRT were independently associated with a thinner SST (regression model: SST=547-0.15×SCT+0.24×SRT+8.8×SER-1.85×age, R²=0.168, P<0.001).

Conclusions: During the early development of myopia, the thinning of the scleral and choroidal tissue in the macular subfoveal region might occur earlier than the retinal thickness. Subfoveal scleral thickness was more responsible for the variation of refractive error than the thickness of the choroid and retina. Age, refractive error, and subfoveal choroidal and retinal thicknesses were the independent related factors of scleral thickness.

Commercial Relationships: Xiangui He, None; Junjie Deng, None; Jiali Jin, None; Minzhi Lv, None; Jianfeng Zhu, None; Haidong Zou, None; Xun Xu, None

Support: 1. Three-year Action Program of Shanghai Municipality for Strengthening the Construction of the Public Health System (2015-2017) (Grant No. GWIV-13.2); 2. National Natural Science Foundation of China for Young Staff (Grant No. 81402695); 3. Key Discipline of Public Health–Eye Health in Shanghai (Grant No. 15GWZK0601)

Program Number: 4429 **Poster Board Number:** A0407

Presentation Time: 11:00 AM–12:45 PM

A 3D MRI study of the relationship between eye dimensions, retinal shape and myopia

David A. Atchison¹, James M. Pope¹, Pavan Verkicharla¹, Farshid Sepehrband¹, Marwan Suheimat¹, Katrina L. Schmid¹, Noel A. Brennan². ¹Institute of Health and Biomedical Innov, Queensland University of Technology, Kelvin Grove, QLD, Australia; ²Johnson & Johnson Vision Care, In., Jacksonville, FL.

Purpose: To investigate changes in overall eye dimensions and in retinal shape with degree of myopia, gender and race.

Methods: There were 58 young adult emmetropes and myopes (range -1.25D to -8.25D), with 30 East-Asians (21 female/9 male), 23 Caucasians (16/7) and 5 South-Asians (1/4). Three-dimensional magnetic resonance imaging was undertaken with a 3.0 Tesla whole-body clinical MRI system using a 4.0 cm receive-only surface coil positioned over the eye. Automated methods determined eye length, width and height, and curve fitting procedures determined asymmetric and symmetric ellipsoid shapes to 75%, 55% and 35% of the retina. Analyses to investigate influence of race and gender were performed with East-Asians and Caucasians.

Results:

With myopia increase, eye dimensions increased in all directions such that increase in length was considerably greater than increases in width and height. Emmetropic retinas were oblate (steepening away from the vertex) but oblateness decreased with increase in myopia, so that retinas were approximately spherical at 7 to 8D myopia. Asymmetry of eyes about the best fit visual axis was generally small, with small differences between the vertex radii of curvature and between asphericities in the axial and sagittal planes. Females had smaller eyes than males, with overall dimensions being about 0.5mm less for the former. Race appeared not to have a systematic effect.

Conclusions: The study confirmed an earlier MRI study, except that meridional differences were smaller. Eyes became less oblate with increasing myopia. Differences between males and females eyes were restricted to overall dimensions rather than shape.

Commercial Relationships: David A. Atchison, None; James M. Pope, None; Pavan Verkicharla, None; Farshid Sepehrband, None; Marwan Suheimat, None; Katrina L. Schmid, None; Noel A. Brennan, Johnson & Johnson Vision Care, Inc. (E)
Support: Johnson & Johnson Vision Care, Inc.

Program Number: 4430 **Poster Board Number:** A0408

Presentation Time: 11:00 AM–12:45 PM

Axial scaling of OCT retinal images is independent of axial length

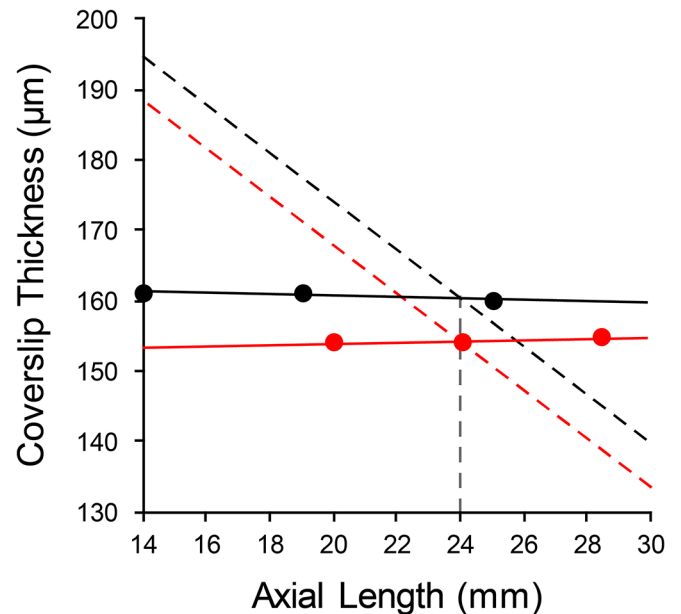
Alexander E. Salmon¹, Benjamin S. Sajdak¹, Ross F. Collery^{1,2}, Joseph Carroll^{1,2}. ¹Cell Biology, Neurobiology, & Anatomy, Medical College of Wisconsin, Milwaukee, WI; ²Ophthalmology & Visual Sciences, Medical College of Wisconsin, Milwaukee, WI.

Purpose: Literature reports¹ of an effect of axial length (AL) on axial scaling in OCT conflict with standard models of axial scaling that are independent of optical power. We sought to investigate the effect of AL on axial scaling and identify the source of the reported effect.

Methods: A model eye was constructed comprising a 19mm lens and a translatable mount housing a glass coverslip at the retinal plane. The AL of the model eye was adjusted (~14-28mm) and the coverslip thickness was measured using the software calipers on a Heidelberg Spectralis OCT/SLO and a Bioptigen Envisu OCT. For the Spectralis, optical power-related eye data (AL, corneal curvature (CC), and refraction) were varied before acquisition of OCT scans to examine possible software sources of axial scaling error. The experiments were repeated with a Spectralis for 3 human subjects with short (AL ≤ 22.5mm), medium (22.5mm < AL ≤ 25.5mm), or long (AL > 25.5mm) eyes, and foveal thickness was measured. Using the Envisu, coverslip thickness was measured as a function of reference arm path length.

Results: Using the model eye, no effect was found between AL and coverslip thickness on the Envisu (Pearson's correlation: $p=0.30$, $R^2=0.79$, $n=3$) or Spectralis ($p=0.32$, $R^2=0.77$, $n=3$; Fig. 1). Thickness measurements were unaffected by varying eye data in the Spectralis software (CC: $p=0.56$, $R^2=0.13$, $n=5$; refraction: 1 μ m difference over a range of 14 diopters). The range of all measurements for 3 model eye ALs, each under 4 AL settings, was 3 μ m compared to the reported 22 μ m for a similar range of ALs.¹ Thickness measurements were unaffected by varying Envisu reference arm path length ($p=0.83$, $R^2=0.0096$, $n=7$). ALs of the human subjects were 22.26mm (short), 24.07mm (medium), and 26.92mm (long), and foveal thickness measurements were unaffected by varying eye data (AL: n-way ANOVA, $p=0.27$, $n=3$; CC: 2-way ANOVA, $p=0.23$, $n=2$; refraction: 2-way ANOVA, $p=1.00$, $n=2$).

Conclusions: Axial scaling in OCT appears to be independent of AL. No explanation of the previously reported effect was found, but software errors were ruled out. Conclusions drawn from reports in which axial scaling was adjusted based on AL should be reevaluated.
¹Röck PMID:25298411



- Bioptigen Envisu (BE)
- Heidelberg Spectralis (HS)
- - - Predicted by Röck from BE @ 24mm
- - - Predicted by Röck from HS @ 24mm

Figure 1. Discrepancy between observed model eye AL/axial scale relationship and previously reported model.

Commercial Relationships: Alexander E. Salmon, None; Benjamin S. Sajdak, None; Ross F. Collery, None; Joseph Carroll, None

Support: T32EY014537, R01EY017607, P30EY001931

Program Number: 4431 **Poster Board Number:** A0409

Presentation Time: 11:00 AM–12:45 PM

Sub-foveal choroidal thickness in myopia and its correlations in central India

Vinay Nangia, Priyanka Pardhi, Sarang Lambat, Ganesh Ambekar. Ophthalmology, Suraj Eye Institute, Nagpur, India.

Purpose: The choroid is involved in retinal pathologies that are sight threatening. It was the purpose to study the choroidal thickness and their correlations in patients of myopia in Central India, where previous data are not available.

Methods: 100 (199 eyes) myopic subjects (53 females) were included. The mean age was 26.65 ± 10.51 yrs. Ocular biometry, fundus photography and spectral domain oct, including enhanced depth imaging of the optic disc and for the choroid was performed. Morphometric parameters of the optic disc, parapapillary atrophy (PPA) and the sub-foveal choroid thickness (SFCT) were measured.

Results: The mean values were for BCVA in DU 0.77 ± 0.27 , spherical equivalent -5.90 ± 3.81 axial length 25.50 ± 1.78 mm. (22.00 - 35.57), and IOP 15.08 ± 2.68 mm.Hg. Mean disc diameter vertical was 1.98 ± 0.77 mm. Mean number of clock hours of PPA (103 eyes) was 6.77 ± 3.63 The maximum width of PPA was 556.91 ± 430 μ m (50-2227). Mean SFCT was 262.71 ± 105 μ m (17-584). For mild myopia ($n=38$) (< 3 D) it was 331.60 ± 105 μ m (103-539) for moderate

myopia (n=94) (3-6D) it was $274.15 \pm 98.16 \mu\text{m}$ (25 - 584) and for high myopia (n=67) (>6D) it was $204.50 \pm 82.86 \mu\text{m}$ (17-368). Bivariate correlations of the SFCT showed significant correlation with age (P=0.001; r=-0.239), male gender (P=0.005; r=0.198), increasing spherical equivalent (P<0.001; r=0.539), BCVA (P<0.001; r=0.478) and vertical disc diameter (P=0.035; r=0.150). SFCT decreased significantly with age (P=0.001; r=-0.239) and increasing axial length (P<0.001; r=-0.581). There was a negative correlation with extent of PPA in clock hours (P<0.001; r=-0.504) and with the maximum width of PPA (P<0.001; r=-0.487). Multivariate analysis with subfoveal choroidal thickness as dependant variable and age, BCVA, axial length, disc diameter vertical, and extent of PPA as independent variables, showed a significant correlation with BCVA (P=0.008), axial length (P=0.004), and extent of PPA (P=0.014).

Conclusions: The values of subfoveal choroidal thickness were determined using Enhanced Depth Imaging with SD-OCT. Increased axial length and greater circular extent of PPA was associated with a thinner choroid. Better BCVA was correlated with a thicker choroid. The study determines the ocular parameters that are associated with choroidal thickness and may play a role in the health of a myopic eye.
Commercial Relationships: Vinay Nangia, None; Priyanka Pardhi, None; Sarang Lambat, None; Ganesh Ambekar, None

Program Number: 4432 **Poster Board Number:** A0410
Presentation Time: 11:00 AM–12:45 PM

Promotion of BMP9/ALK1 quiescence signaling for the prevention of Diabetic Macular edema

Naoufal N. Akla^{1,3}, Claire Viaillard³, Ali Belayachi³, Bruno Larrivee^{2,3}. ¹Biochemistry and molecular medicine, Université de Montréal, Montreal, QC, Canada; ²Ophthalmology, Université de Montréal, Montreal, QC, Canada; ³Hopital Maisonneuve-Rosemont, Montreal, QC, Canada.

Purpose: Sight-threatening diabetic macular edema (DME) is caused by increased microvascular permeability. While few direct vascular targeting strategies are available, VEGF pathway inhibition has shown to be effective in reducing retinal vascular leakage but is associated with non-negligible side effects. Thus more options are needed. Vascular specific Activin-like kinase receptor type I (ALK1) pathway and its circulating ligand Bone morphogenetic protein-9 (BMP9) is known for its potent quiescent and stabilizing effect on the vasculature. However, little is known about this pathway in the context of microvascular permeability associated with diabetes. We hypothesize that BMP9/ALK1 pathway is inhibited in diabetic (DB) retinas leading to vascular destabilization and leakage and that its activation could re-establish proper vascular endothelial barrier functions (EBF).

Methods: The effect of hyperglycemia (i.e. HG>10 mM of D-glucose) on Alk1 signaling was evaluated in vitro by subjecting endothelial cells (EC) to increasing concentrations of D-glucose (5, 11, 25 mM) and *In vivo* using DB mice (Streptozotocin-induced diabetes). [B1] The contribution of Alk1 signaling on EBF was evaluated using Evans Blue permeation in inducible endothelial specific Alk1 KO mice. To evaluate the potential protective effects of BMP9/Alk1 signaling on EBF, BMP9 overexpression was achieved using adenoviral delivery in DB mice. Statistical-One-Way ANOVA or Student's t-test was used.

Results: Endothelial tissue from DB mice showed a significant inhibition of BMP9/ALK1-canonical Smad1,5,8 quiescence signaling (DB n=5; CTL n=4; p<0.01), which was associated with reduced expression of target genes (JAG1, Id1,3, Hey1,2 & HES). Moreover, we showed that retinal hyperpermeability associated with diabetes

was exacerbated in Alk1 heterozygote mice (n=4-9/group; p<0.0001). Finally, we demonstrated that activation of Alk1 signaling in ECs prevented vascular permeability induced by HG, both *In vitro* (n=3; p=0.009) and *In vivo* (n=4-9/group; p<0.0001).

Conclusions: Consistent with our hypothesis, vascular stability and quiescence induced by BMP9-ALK1 signaling is inhibited in the DB/HG endothelium, which could be an important factor in vascular leakage leading to DME. Our results show that activation of this pathway could offer a therapeutically interesting future option to slow down the onset of DME.

Commercial Relationships: Naoufal N. Akla, None; Claire Viaillard, None; Ali Belayachi, None; Bruno Larrivee, None

Support: Heart and Stroke Foundation of Canada

Program Number: 4433 **Poster Board Number:** A0411

Presentation Time: 11:00 AM–12:45 PM

Changes in Macular Retinal Thickness During Emmetropization and Myopia Development in Juvenile Marmosets

Harrison Feng, Xiaoying Zhu, Ann Nour, Rita Nieu, Alexandra Benavente-Perez. SUNY College of Optometry, New York City, NY.

Purpose: To describe the structural macular retinal thickness changes that occur in juvenile marmosets as a function of age and compared to those in marmosets that developed myopia.

Methods: Refractive error (Rx), axial length (AL), and sub and parafoveal retinal thickness (RT, 0.5-3.0mm from foveal pit, 360 deg) were measured in 13 marmosets (N=7 treated with -5D; N=6 age-matched controls) from 10 to 20 weeks of age using the Nidek autorefractor, a high frequency A-scan ultrasound and the Bioptigen Spectral Domain Optical Coherence Tomography (SD-OCT) respectively. Ultrasound and square volume SD-OCT (12x12mm, 100 B-scans, 1000 A-scans/B-scan) were performed under anesthesia (alfaxan, 1.5mg/kg, im). Retinal thickness (RT) was quantified using The Iowa Reference Algorithms v3.6 (Iowa Institute for Biomedical Imaging).

Results: With age, the eyes of control marmosets emmetropized with a slight overall retinal thickening (change in Rx, AL and average RT, mean±SE: -1.74±1.02D, 0.67±0.03mm, 5.07±6.88µm). The temporal and superior quadrants thickened at a faster rate than the inferior and nasal regions (12.06±5.49, 9.72±5.85, 7.54±5.43 and 2.02±6.70µm respectively, p>0.05). In all quadrants except in the superior, the age-related retinal thickening decreased with eccentricity. Prior to treatment, the retinas of animals that were larger in size were also thinner on the inferior and nasal region closer to the ONH (R=-0.59, p<0.05; R=-0.50, p=0.08 respectively). After treatment, -5D treated eyes grew faster and developed myopia (change in Rx and AL: -5.87±1.24D, 0.95±0.04mm), and also experienced an overall retinal thickening (change in RT; temporal: 16.27±7.40, superior: 9.11±7.06, inferior: 6.00±4.43, nasal: 4.58±7.39µm respectively, p>0.05). In these myopic eyes, the inferior outermost region thickened at a slower rate as eyes grew longer (R=-0.74, p=0.09).

Conclusions: Retinal thickness can be safely and reliably measured non-invasively *in-vivo* in marmosets under anesthesia. As it occurs in infant human eyes, the overall subfoveal and parafoveal retina of marmosets thickens with age. Within each quadrant, the parafoveal retina thickening decreased with eccentricity. Marmoset eyes that developed myopia and grew at a faster rate experienced a slight slower age-related thickening of the inferior retina, possibly suggesting early anatomical differences during myopia development.

Commercial Relationships: Harrison Feng, None; Xiaoying Zhu, None; Ann Nour, Johnson and Johnson Vision Care, Inc (F);

Rita Nieu, None; Alexandra Benavente-Perez, Johnson and Johnson Vision Care, Inc (F)

Program Number: 4434 **Poster Board Number:** A0412

Presentation Time: 11:00 AM–12:45 PM

Retinal and Choroidal Thickness Measurements – Repeatability and Influence of Axial Length

Hannah Burfield, Ashutosh Jnawali, Nimesh B. Patel, Lisa A. Ostrin. University of Houston College of Optometry, Houston, TX.

Purpose: The choroid is a dynamic vascular structure that has been implicated in eye growth regulation and myopia development. Evidence suggests that the choroid modulates thickness in response to defocus and chromatic cues, and may differ in emmetropic and myopic individuals. The goal of this study was to evaluate choroidal thickness across the posterior pole and examine the relationship with axial length.

Methods: Right eyes of 30 subjects (ages 21–40) were imaged with spectral domain optical coherence tomography (SD-OCT) using six 30° radial scans centered at the fovea. All measurements occurred between 9:00–10:00 am, and were repeated at the same time within two weeks. Following OCT, cycloplegic autorefractometry and axial length (AL) were measured. OCT images were analyzed using a custom written program in Matlab after adjusting for lateral magnification. Scans were segmented for the inner limiting membrane, Bruch's membrane and posterior choroid. Retinal (RT) and choroidal thickness (CT) were determined for the fovea and subfovea, central 1mm diameter, and 3mm and 6mm annular rings.

Results: Emmetropic subjects (n=14, SE 0 ± 0.4 D) had a central RT of 219.7 ± 17.8 µm and CT of 382.4 ± 81.6 µm, and myopic subjects (n=16, -3.6 ± 1.9 D) had a central RT of 225.1 ± 20.6 µm and CT of 307.7 ± 78.6 µm, respectively. Regression analyses showed that foveal RT increased with AL (p < 0.05); however, 1mm, 3mm, and 6mm regions were not correlated. Subfoveal CT, 1mm diameter, and 3mm and 6mm annuli significantly decreased with increasing AL and myopic refraction (p < 0.05 for all). For all subjects, the retina was thickest in the superior and nasal regions, and the choroid was thickest in the temporal and inferior regions. Bland-Altman analyses revealed an average difference of -1.4 ± 16.5 µm for subfoveal CT and 0.6 ± 3.9 µm for foveal RT.

Conclusions: Results show that the choroid is significantly thinner with longer axial length, including central and peripheral regions. Retinal thickness significantly increased with longer axial length in the foveal region only. Differences in CT and RT with axial length could be a consequence of biomechanical or developmental changes. SD-OCT was shown to be capable of wide-field retinal and choroidal imaging with good repeatability, and can be further used to examine the role of the choroid in eye growth and myopia development.

Commercial Relationships: Hannah Burfield, None; Ashutosh Jnawali, None; Nimesh B. Patel, None; Lisa A. Ostrin, None

Support: T35EY007088

Program Number: 4435 **Poster Board Number:** A0413

Presentation Time: 11:00 AM–12:45 PM

Influence of Body Position in Intraocular Pressure and Lens Vault in Healthy Eyes

Handan AKIL¹, Vikas Chopra^{1,2}, Brian A. Francis^{1,2}, Srinivas R. Sadda^{1,2}, Alex S. Huang^{1,2}. ¹Doheny Imaging Reading Center, Doheny Eye Institute, Los Angeles, CA; ²Ophthalmology, David Geffen School of Medicine, University of California Los Angeles, Los Angeles, CA.

Purpose: Changes in body position from upright to supine are known to be associated with a rise in intraocular pressure (IOP). In this study

of healthy eyes, we investigate position-related changes to anterior chamber morphology, in particular lens vault.

Methods: Fourteen eyes were recruited for this prospective, IRB-approved study. The participants were asked to remain seated for 10 minutes and then had their baseline IOP measured with a pneumatonometer followed by anterior segment OCT. The subjects then assumed a supine position for 10 minutes again followed by IOP measurement and anterior segment OCT. OCT images were taken with the Spectralis HRA+OCT (Heidelberg Engineering GmbH) using the two-angle anterior segment horizontal scan centered on the pupil (ART = 60). To image in multiple positions, the Spectralis FLEX module was used. The FLEX module is a modified surgical boom arm that orientates the Spectralis for imaging in nearly any body position. For image analysis, lens vault was defined as the perpendicular distance between the anterior pole of the crystalline lens to a horizontal line joining the 2 scleral spurs, on horizontal anterior-segment OCT B-scans. Anterior chamber width was also calculated and defined as the horizontal distance between the two scleral spurs. Statistical analysis was used to evaluate positional changes in intraocular pressure and lens vault.

Results: The mean age was 36.5±5.6 years. The spherical equivalent of the eyes was -2.5±1.3. IOP measured in the seated position was 17.65±2.7 mm Hg, and 23.2±2.2 mm Hg when the subjects were in a supine position (p = 0.01). Lens vault was -28.14±176.265 µm in the seated position and -258.93±251.54 µm in the supine position (p = 0.04). There was no statistically significant difference between two positions for the anterior chamber width (p=0.3).

Conclusions: Comparison of positional variations in anterior chamber anatomy as measured by OCT has recently become possible with the advent of the FLEX module. This study found that both IOP and positional changes in anterior chamber anatomy can occur in normal healthy eyes. Understanding normal positional anatomic changes may provide new insights into disease pathophysiology.

Commercial Relationships: Handan AKIL; Vikas Chopra, Allergan (C), Allergan (F); Brian A. Francis, Neomedix (C), BVI Endoptiks (C), Lumenis (F), Innofocus (F), Aquesys (F), Diopsys (F), Allergan (F); Srinivas R. Sadda, Novartis (C), Optos (C), Allergan (F), Carl Zeiss Meditec (F), Genentech (C), Thrombogenics (C), Optos (F), Genentech (F), Iconic (C), Allergan (C); Alex S. Huang, Heidelberg Engineering (F), Allergan (C)

Program Number: 4436 **Poster Board Number:** A0414

Presentation Time: 11:00 AM–12:45 PM

Morphological Ciliary Muscle Changes Associated with Form Deprivation Myopia in the Guinea Pig

Andrew D. Pucker¹, Ashley R. Jackson², Kirk M. McHugh^{3,2}, Donald O. Mutti⁴. ¹Optometry, University of Alabama at Birmingham, Birmingham, AL; ²Center for Molecular and Human Genetics, Nationwide Children's Hospital, Columbus, OH; ³Department of Biomedical Education & Anatomy, The Ohio State University, Columbus, OH; ⁴Optometry, The Ohio State University, Columbus, OH.

Purpose: Myopic subjects are known to have larger posterior ciliary muscle than non-myopic subjects, though the field currently lacks an animal model for studying this relationship. The purpose of this study was to investigate whether form deprivation-induced myopia in guinea pigs results in morphological changes in the ciliary muscle similar to the thickening seen in human myopia.

Methods: Nineteen guinea pigs were bred from in house progenitors obtained from Cincinnati Children's Hospital (unknown strain) and the United States Army (Strain 13). At 2-3 days of age the right eyes of animals were treated with translucent occluders for 7 days while the left eyes served as controls. Refractive error and vitreous chamber

depth (VCD) measurements were determined with retinoscopy and A-scan ultrasonography, respectively. Ciliary muscle dimensions were determined histologically by fluorescently labeling smooth muscle cells (anti- α -smooth muscle actin conjugated with FITC) and cell nuclei (Draq5) and quantitatively analyzing ciliary muscle characteristics with Stereo Investigator (MBF Bioscience). Animals were considered responsive to treatment if they had anisometropia > -2.00 D and VCD differences > 0.1 mm.

Results: Eight responsive animals (4 of each strain) were obtained and analyzed. On average responsive animals had (mean \pm SD of right minus left eyes; 95% confidence interval) ciliary muscle lengths (720.24 \pm 98.92 μ m vs. 753.61 \pm 91.37 μ m; 47.30, -114.04), cross-sectional areas (0.045 \pm 0.01 mm² vs. 0.052 \pm 0.02 mm²; 0.001, -0.016), cell numbers (185.63 \pm 43.05 cells vs. 213.41 \pm 77.60 cells; 16.05, -71.61), and cell sizes (244.02 \pm 22.83 μ m²/cell vs. 250.23 \pm 23.77 μ m²/cell; 17.95, -30.36) that were smaller in the treated eyes compared to the control eyes. The unresponsive animals had no clear growth trends for any ciliary muscle measurement (all confidence intervals included zero).

Conclusions: This study found no evidence that form deprivation-induced myopia resulted in ciliary muscle hypertrophy even though form deprivation resulted in longer, myopic eyes. While additional animals are needed to fully investigate if a relationship truly exists, the results of this study suggest that induced myopia does not promote, and may actually inhibit, ciliary muscle growth, opposite in direction to that seen in human juvenile myopia.

Commercial Relationships: Andrew D. Pucker, None;

Ashley R. Jackson, None; Kirk M. McHugh, None;

Donald O. Mutti, None

Support: NIH/NEI: K08EY023264

Program Number: 4437 **Poster Board Number:** A0415

Presentation Time: 11:00 AM–12:45 PM

Interactions between paired eyes during normal growth and lens compensation in chicks

Xiaoying Zhu^{1,2}, Sally A. McFadden². ¹Biological and Vision Sciences, State University of New York, College of Optometry, New York, NY; ²School of Psychology, University of Newcastle, Callaghan, NSW, Australia.

Purpose: Many animal studies have shown that monocular optical treatment on one eye (either form deprivation or lens treatment) can affect the contralateral untreated eye, in terms of change in refractive error, ocular dimensions, and in certain molecular pathways:

Monocular treatment on the treated eye can cause the contralateral eye to change either in the same direction as the treated eye (yoking) or the opposite direction (anti-yoking; Rucker *et al.*, 2009, ARVO E-abstract 3931). We undertook a meta-analysis of the interactions (symmetrical size, symmetrical growth, yoking, and anti-yoking) in axial length (AL) in both untreated normal eyes and chicks wearing a spectacle lens on one eye.

Methods: (1) AL from both eyes in untreated chicks (n = 3008) was obtained to study the correlation between paired eyes and changes with age (1-17 days). (2) Another group of untreated chicks (n = 48) were measured on days 7 and 10 to study the AL growth in paired eyes. (3) Chicks wore spectacle lenses of various powers (+/- 5, 7, 10, and 15 D, n = 169) over one eye for various durations (1 to 7 days) and were measured before and after the treatment. The change in AL in the fellow eyes was compared to that estimated from eyes of age-matched untreated animals.

Results: (1) The AL in paired eyes was highly correlated, suggesting symmetrical size, and there was a linear relationship between AL and age ($y = 0.065x + 8.39$ mm, from 1 to 17 days of age; $r^2 = 0.36$, $p < 0.0001$). (2) The change in AL in paired eyes was also highly

correlated ($y = 0.69x + 0.07$ mm, $r^2 = 0.56$, $p < 0.0001$), suggesting symmetrical growth. (3) Both yoking and anti-yoking were observed after positive and negative lens treatments. Yoking effects increased with longer lens-wear durations for both positive and negative lens treatment, and dominated anti-yoking effects which were inconsistently observed and only when the lens-wear period was short.

Conclusions: Eye growth in untreated chicks was tightly regulated, shown with both symmetrical size and growth. While the exact mechanisms are unknown, monocular spectacle lens treatment caused both yoking and anti-yoking in the contralateral eyes. In monocular experiments, anti-yoking might sometimes lead to erroneous conclusions if comparisons are relative to the fellow eye, but such effects can be easily overcome by increasing the lens-wear period to greater than 4 days.

Commercial Relationships: Xiaoying Zhu, None;

Sally A. McFadden, None

Program Number: 4438 **Poster Board Number:** A0416

Presentation Time: 11:00 AM–12:45 PM

A dose dependent myopic shift in refraction and axial length in a murine model of lens-induced myopia

Xiaoyan Jiang^{1,2}, Kiwako Mori^{1,2}, YASUHISA TANAKA^{1,2}, Shin-ichi Ikeda^{1,2}, Maki Miyauchi^{1,2}, Erisa Yotsukura^{1,2}, Hidemasa Torii^{1,2}, Toshihide Kurihara^{1,2}, Kazuo Tsubota¹.

¹Department of Ophthalmology, Keio University School of Medicine, Tokyo, Japan; ²Laboratory of Photobiology, Keio University School of Medicine, Tokyo, Japan.

Purpose: The global increase of myopia is becoming a serious health hazard in the world. To investigate the molecular mechanism of the disease pathogenesis, it is desirable to induce axial elongation in mice with an efficient and effective method in terms of genetic manipulation. Here we show a highly reproducible murine lens-induced myopia (LIM) model and investigate the adaptability of mouse eye to different optical power lenses.

Methods: Frames of the eyeglasses for the murine (LIM) were designed according to the shape of the mouse head, and were made of titanium produced by a 3D-printer. Plus 5 diopter (D), negative 10D, 20D, and 30D lenses made of PMMA were fixed to the right eye side of the frame (n=5 each) and plano 0D lenses were fixed to the left eye side as internal controls. 3-week-old wild-type C57BL/6J mice were attached the eyeglasses by mounting the frame on their skull using a self-cure dental adhesive system. An infrared photorefractor (Steinbeis Transfer Center, Germany) was used to measure the refractive state. The axial length of the eye was analyzed by a SD-OCT system (Envisu R4310, Leica, Germany) under general anesthesia by the combination of midazolam, medetomidine and butorphanol tartrate (MMB).

Results: After three weeks of lens wearing, significant lens power dependencies were observed in both refraction changes (D, control eyes vs affected eyes, average \pm standard deviation; +5D group: 7.18 \pm 7.67 vs 10.64 \pm 8.15, $p=0.5$; -10D group: 6.86 \pm 9.76 vs -15.70 \pm 2.54, $p=0.001$; -20D group: 3.15 \pm 5.13 vs -22.19 \pm 6.12, $p=0.0001$; -30D group: -1.31 \pm 3.84 vs -26.66 \pm 10.86, $p=0.0001$) and axial length changes (mm, control eyes vs affected eyes, average \pm standard deviation; +5D group: 0.25 \pm 0.05 vs 0.27 \pm 0.05, $p=0.72$; -10D group: 0.22 \pm 0.02 vs 0.25 \pm 0.04, $p=0.26$; -20D group: 0.24 \pm 0.02 vs 0.27 \pm 0.03, $p=0.07$; -30D group: 0.19 \pm 0.01 vs 0.25 \pm 0.02, $p=0.01$).

Conclusions: The axial length with -30D lenses was changed more significantly than -20D and -10D lenses according to SD-OCT measurements although the mouse eyes were not fully compensable with -30D lenses. Dose dependent myopia due to lens power was confirmed in our murine LIM model.

Commercial Relationships: Xiaoyan Jiang, None; Kiwako Mori, None; YASUHISA TANAKA, None; Shin-ichi Ikeda, None; Maki Miyauchi, None; Erisa Yotsukura, None; Hidemasa Torii, None; Toshihide Kurihara, None; Kazuo Tsubota, None

Program Number: 4439 **Poster Board Number:** A0417
Presentation Time: 11:00 AM–12:45 PM

Quantitative 3-D OCT ocular geometry of lens-treated myopic and hyperopic guinea pig eyes

Pablo Perez-Merino¹, Eduardo Martinez-Enriquez¹, Miriam Velasco-Ocana¹, Luis Revuelta², Susana Marcos¹, Sally A. McFadden³.

¹Instituto de Optica-CSIC, Madrid, Spain; ²Universidad Complutense, Facultad de Veterinaria, Madrid, Spain; ³University of Newcastle, School of Psychology, Newcastle, NSW, Australia.

Purpose: Animal models of myopia traditionally emphasize the changes in posterior parameters of the eye and associated elongation. Less attention has been paid to potential optical changes, so we evaluated 3D corneal and crystalline lens geometry in myopic and hyperopic guinea pig eyes following monocular lens treatment.

Methods: Guinea pigs wore either a -6D (n=4) or a +5D (n=3) lens on one eye from 4-13 days of age. After 8 days of lens-wear, each eye was measured in anaesthetized animals using 3-D spectral OCT (300 Ascans x 50 Bscans in a 8x8 mm area; acquisition speed: 25.000 Ascans/s). OCT-images were obtained in two foci: (1) full anterior segment, (2) posterior lens and retina. The following parameters were extracted using custom-developed image processing and quantification routines: radii of curvature for the anterior and posterior corneal and crystalline lens (Rant/post C/L), asphericities (Qant/post C/L) and elevation maps (surface Zernike coefficients), corneal and lens thickness (CT, LT), anterior and vitreous chamber depths (ACD, VCD). Volume (VOL), Diameter (DIA) and equatorial plane position (EPP) of the lens were estimated from full reconstructions from partial images. Refractive error was measured in cycloplegic eyes using streak retinoscopy.

Results: The mean difference between the eyes (diff) in refractive error was -6.03D after minus lens wear and +1.53D after positive lens wear, and was accompanied by longer or shorter VCDs respectively (diff: +230 Vs. -56 µm). Bidirectional changes also occurred in the corneal radii, becoming steeper after negative and flatter after positive lens-wear (diff in myopes: -130 µm and -51µm (ant), diff in hyperopes: +106 µm and +19 µm (post)). The crystalline lens was thicker and had a greater volume after negative lens wear (diff of 30 µm and 1.2 mm³ respectively). The magnitude of astigmatism was x3.5 (ant cornea) and x2.6 (posterior lens) higher in the myopic eyes in comparison with the hyperopic eyes; higher-order RMS surface elevation was largest in the posterior lens of the myopic eyes (x2.2; vertical coma was the dominant coefficient).

Conclusions: Sign dependent changes were observed in the corneal radius and the vitreous chamber depth, and significant changes occurred in the crystalline lens. Therefore, exposure to retinal defocus systematically changes the optical properties of the developing eye.

Commercial Relationships: Pablo Perez-Merino, None;

Eduardo Martinez-Enriquez, None; Miriam Velasco-Ocana, None; Luis Revuelta, None; Susana Marcos, WO2012146811A1 (P); Sally A. McFadden, None

Support: FIS2014-56643; FIS2011-25637; ERC-2011-AdG-294099; G1400967 HMRI

Program Number: 4440 **Poster Board Number:** A0418

Presentation Time: 11:00 AM–12:45 PM

In Vivo Imaging of Blood Vessel Regression in Retinal Degeneration

Joseph Hanna¹, Neeru Gupta^{1,2}, Xun Zhou¹, Emily Mathieu^{1,2}, Luz A. Paczka-Giorgi¹, Yeni H. Yucel^{1,2}. ¹Keenan Research Centre for Biomedical Science, St. Michael's Hospital, Toronto, ON, Canada; ²Laboratory Medicine and Pathobiology, Ophthalmology and Vision Sciences, University of Toronto, Toronto, ON, Canada.

Purpose: To non-invasively evaluate the retinal vessels of the Tie2-GFP mouse strain in vivo.

Methods: Homozygous (hm) Tie2-GFP mice retinas (JAX, USA) expressing green fluorescent protein (GFP) in their vascular endothelium with known retinal degeneration, were studied. Hm mice were crossed with CD1 mice (Charles River Laboratories, Canada) generating control heterozygous (ht) Tie2-GFP mice. Retinas of 12 (6M, 6F) hm Tie2-GFP were evaluated at 2 weeks (n=4), 3 months (n=4) and 8 months (n=4), and compared to control ht Tie2-GFP mice at the same time points (6M, 6F, n=12). Under isoflurane anesthesia, mouse retinas were imaged using blue Autofluorescence funduscopy (3 and 8 months) and 3D Optical Coherence Tomography (Spectralis, Heidelberg Engineering, Germany). 3D OCT was used to compare retinal thicknesses of hm and control mice. Histopathological validation was performed with isolectin/DAPI stained sections (Invitrogen, USA), imaged by confocal microscopy. Retinal thickness measured using OCT was compared between groups using *t*-test.

Results: At 3 months, in vivo blue autofluorescent funduscopy of hm Tie2-GFP mice showed fewer branching vessels compared to ht controls. (Fig. 1A-B). At 8 months, Tie2-GFP signal was not observed in main or branching vessels, compared to controls. At all-time points, retinal thicknesses of hm mice were significantly reduced compared to ht controls, with mean thicknesses of (163±6.6µm vs. 250.1±16µm), (94.3±8µm vs. 207.4±7.3µm) and (85.4±7.3µm vs. 208.75±7.8µm) (p<0.001) at 2 weeks, 3 and 8 months, respectively.

At 2 weeks, Isolectin sections showed normal inner retinal vasculature in both hm mice and controls. At 3 months, hm mice retinas showed loss of deep vascular plexus, with degeneration of the photoreceptor and outer nuclear layers compared to age-matched ht controls. By 8 months, decreased isolectin staining had extended from the deep vascular plexus to intermediate and superficial plexuses compared to age-matched controls.

Conclusions: Non-invasive retinal imaging of a widely used hm Tie2-GFP mouse model showed blood vessel regression extending from deep to superficial plexuses. Further studies are needed to explore pathways and potential therapies to target angio-regression in retinal degenerations.

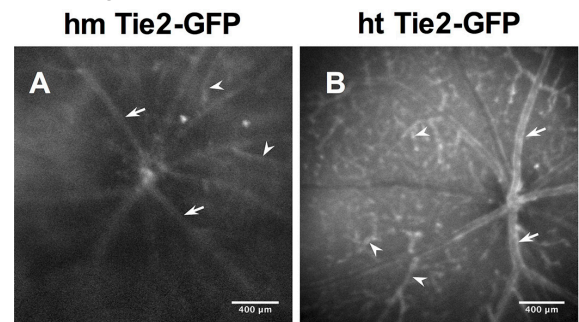


Figure 1. Fundus scans of homozygous (hm) Tie2-GFP mouse at 3 months shows reduced signal in main (arrows) and branching (arrowheads) vessels (A) compared to heterozygous (ht) control mouse (B).

Commercial Relationships: Joseph Hanna, None; Neeru Gupta, None; Xun Zhou, None; Emily Mathieu, None; Luz A. Paczka-Giorgi, None; Yeni H. Yucel, None

Support: Nicky and Thor Eaton Research Fund, Canada Foundation for Innovation Grant 31326, Henry Farrugia Research Fund